15 (2022) 100169

Contents lists available at ScienceDirect

International Journal of Thermofluids

journal homepage: www.sciencedirect.com/journal/international-journal-of-thermofluids

Synthesis and characterization of goethite (α-FeOOH) magnetic nanofluids

Maria Raffaella Martina [a], Luca Zoli [b], Elisa Sani [a,*]

[a] CNR-INO National Institute of Optics, Largo E. Fermi, 6, Firenze 50125, Italy
[b] CNR-ISTEC, Institute of Science and Technology for Ceramics, Via Granarolo 64, Faenza 48018, Italy

ARTICLE INFO

Keywords:
Magnetic nanofluids
Ferrofluids
Goethite
Optical properties

ABSTRACT

Magnetic nanofluids consisting of goethite nanoparticles in aqueous suspensions have been successfully synthesized using two sodium-free routes. Nanoparticle morphology, nanofluid stability and optical properties have been studied and compared with a goethite nanofluid whose nanoparticles are synthesized with a different protocol using NaOH. The synthesis procedure determines the nanoparticle size and morphology, which, in turn, is connected to optical properties and their sensitivity to external magnetic fields. The highest sensitivity is shown by the sample synthesized with NaOH, which is characterized by the largest nanoparticles (261±5 nm hydrodynamic size) and whose absolute transmittance values increase or decrease by about 11% and 20%, respectively, depending on to the mutual directions of magnetic field and electromagnetic wave polarization/wave vector, for an applied magnetic field of 5.60 mT. Nanoparticles in the fluid are therefore able to discriminate both the absolute value and the direction of the magnetic field and, moreover, being their response non-spectrally flat, specific spectral ranges exist where their response is maximized.

Introduction

Goethite (α-FeOOH) is a common and stable iron oxide present in natural environment and so far has been extensively investigated for several applications including, only to mention few of them, water purification [1], organic pollutant degradation [2], coatings, pigments [3], by virtue of its chemical stability, nontoxicity and low cost [4]. Goethite nanoparticles commonly take the form of needle-like structures, naturally asymmetric and anisotropic and with antiferromagnetic properties. These characteristics influence the direction and orientation of goethite nanoparticles as a function of the intensity and direction of an externally applied magnetic field [5,6]. For instance, Lemaire et al. widely investigated aqueous suspensions of goethite nanorods giving rise to stable isotropic and nematic phases showing peculiar magnetic properties because goethite nanorods align parallel to a weak magnetic field but perpendicular to a strong field [7,8] due to a permanent longitudinal magnetic moment along the elongated axis, probably due to uncompensated surface spins within the anti-ferromagnetic crystal structure [4].

The use of magnetic nanoparticles in nanofluids (also called ferrofluids in the specific case), have recently gained increased interest in different application fields, such as electrical and thermal engineering [9–13], medicine and biology [14,15], sensing and optical devices [16, 17]. Recently, a ferrofluid containing Fe_3O_4 nanoparticles has been tested in a linear parabolic solar collector in the Direct Absorption Solar Collector (DASC) scheme [18], i.e. with the ferrofluid carrying out both the direct sunlight absorption and the heat transfer functions. This produced an efficiency increase with respect to the conventional collector architecture, also taking benefit from the magnetic-field enhancement of ferrofluid thermal conductivity. Moreover, magnetic maghemite-nanofluids (γ-Fe_2O_3) have been investigated in novel thermoelectric cells based on liquid electrolytes [19,20], obtaining promising results.

The application of a magnetic field adds a degree of freedom to manipulate the properties of magnetic nanoparticles and of the systems where they are used [21]. It also allows recovering nanoparticles after use, boosting their overall safety, recyclability and sustainability. However, the specific behavior under applied magnetic field depends on the concentration, shape and size of the nanoparticles [22], as well as on the magnetic field characteristics themselves. Deepening the correlation between magnetic orientation and morphology of nanoparticles can pave the way for new applications in key sectors, like the biomedical field for personalized therapy and drug delivery, and environmental applications for magnetic-field sensors, removal of metal pollutants from contaminated environments, etc.

Morphological and structural characteristics of magnetic goethite

* Corresponding author.
E-mail address: elisa.sani@ino.cnr.it (E. Sani).

https://doi.org/10.1016/j.ijft.2022.100169

Available online 9 June 2022

nanoparticles (e.g., microstructures, sizes and aggregation state) are influenced by the synthesis method [6,23,24]. Therefore, in this work, we experimented with different approaches for the synthesis of goethite nanoparticles and we explored the optical, magnetic and morphological properties of the obtained nanostructures. To this aim, three synthesis routes have been explored changing for aging temperatures and times, pH and use of organic or inorganic alkali to monitor the properties of different goethite nanoparticles in water suspensions.

Experimental

Goethite (α-FeOOH) nanoparticles (mw=88.85 g/mol) have been synthesized by the aging of ferrihydrite suspensions obtained through co-precipitation (sample #1 and sample #2) and by a process based on the fast conversion of ferrihydrite through ultrasonic irradiation (sample #3).

In all synthesis routes, Fe $(NO_3)_3{\cdot}9H_2O$ (>98% pure by Alfa Aesar, Thermo Fisher Scientific) has been used as metal oxide precursor and deionized water (for analysis EMSURE®, Merck) was used as solvent. Approximate goethite concentrations have been estimated as follows: for sample #1, the mass concentration has been measured from sample drying, followed by rehydration and redispersion by repeated ultrasonic irradiation cycles of the sample in an aqueous environment. For samples #2 and #3, the concentration has been estimated comparing their optical spectra with those of sample #1. It should be pointed out that these concentrations have to be considered as a rough estimation, as errors can arise from the presence of a residual percentage of iron oxide precursor not converted into goethite, and from morphology-dependent features in the spectra. However they can be taken as indicative of the order of magnitude of concentrations and their qualitative differences among samples.

Sample #1 has been prepared by adding dropwise 5 mL of 0.06 M Fe $(NO_3)_3$ solution to 45 mL of 1.5 M NaOH solution at room temperature. NaOH (anhydrous pellets, by JY Baker) has been used to prepare the co-precipitation solution. A ferrihydrite precipitate was obtained which was aged afterwards 3 days. The aging period resulted in the conversion of ferrihydrite in goethite precipitate which has been washed several times with water followed by centrifugation and pH adjustment. The stable colloids have been obtained by proper dilution and 60 min ultrasound irradiation operating at 40 kHz and 180 W operated at 80% power. Estimated goethite concentration was 0.6 mg/ml derived from drying test, as described above.

Sample #2 follows the same synthesis procedure as #1, except for the dropwise addition of an organic alkali instead of NaOH, in particular 35 wt% tetra-ethylammonium hydroxide (TEAH) water solution (by Alfa Aesar, Thermo Fisher Scientific) to 20 mL of 0.1 M $Fe(NO_3)_3$ solution at room temperature. The sample was aged in an oven for 24 h, followed by washing and centrifugation. Estimated goethite concentration of sample #2 was 0.3 mg/ml.

Sample #3 has been prepared by adding all at once 35 wt% TEAH water solution (5 mL) to 20 mL of 0.1 M $Fe(NO_3)_3$ solution at room temperature, leading to a ferrihydrite precipitate. The mixture has been treated subsequently by ultrasound irradiation for 1 h at 30 °C. Estimated goethite concentration in this sample was 0.2 mg/ml.

A Malvern Zetasizer Nano 3600 was used to investigate the size distribution within the colloids exploiting the dynamic light scattering (DLS) technique.

Scanning Electron Microscopy (FE-SEM, Carl Zeiss Sigma NTS Gmbh, Oberkochen, DE) and energy dispersive x-ray spectroscopy (EDS, INCA Energy 300, Oxford instruments, UK) characterizations were carried out. EDS was calibrated with a cobalt standard and INCA internal procedure for semi-quantitative analysis. Suspensions were observed by evaporating a drop of them on a holey carbon film coated copper grid (300 mesh).

Optical transmittances in the UV–Vis–NIR range from 300 to 1500 nm have been determined both in absence of magnetic field and under different magnetic field intensities and directions with respect to light polarization using a Perkin-Elmer Lambda900 spectrometer equipped with Glan-Thompson polarizers. The spectral resolution was 2 nm. Different values of magnetic field were created during optical measurements using permanent magnets. The magnetic field was measured using a Bell 640 Incremental Gaussmeter and a transverse probe 5 mm large and 1 mm thick. The probe was located at the point of optical measurements.

Results

The goethite nanoparticles were synthesized in stable aqueous suspensions and showed rod-like morphologies with length of about 200 nm and thickness of a few tenths nm, stacked into nematic arrangement [6].

The following reactions are reported by Cudennec and Lecerf to highlight the mechanism of formation of ferrihydrite, a poorly crystalline oxide, of rough formula $5Fe_2O_3{\cdot}9H_2O$ after pH modification of cationic iron water solution and goethite, α-FeO(OH) after aging at pH >10 [25]:

$$Fe(NO_3)_3 \Rightarrow^{water} {\cdot}Fe^{3+}_{(aq)} + 3NO^{-}_{3\,(aq)};\ Fe^{3+}_{(aq)} \equiv \left[Fe(OH_2)_6\right]^{3+} \quad (1)$$

$$\left[Fe(OH_2)_6\right]^{3+} + H_2O \rightleftarrows \left[Fe(OH_2)_5OH\right]^{2+}_{(aq)} + H_3O^{+} \quad (2)$$

$$\left[Fe(OH_2)_5OH\right]^{2+}_{(aq)} + OH^{-} \rightleftarrows \left[Fe(OH_2)_4(OH)_2\right]^{+}_{(aq)} \quad (3)$$

$$\left[Fe(OH_2)_4(OH)_2\right]^{+}_{(aq)} + OH^{-} \rightleftarrows \left[Fe(OH_2)_3(OH)_3\right]_{(s)}\downarrow \quad (4)$$

$$[5Fe_2O_3{\cdot}9H_2O] + 10OH^{-} + 26H_2O \rightleftarrows 10\left[Fe(OH_2)_2(OH)_4\right]^{-}_{(aq)} \quad (5)$$

$$\left[Fe(OH_2)_2(OH)_4\right]^{-}_{(aq)} + OH^{-} \rightleftarrows \left[Fe(OH_2)(OH)_5\right]^{2-}_{(aq)} \rightarrow + H_2O \quad (6)$$

$$\left[Fe(OH_2)(OH)_5\right]^{2-}_{(aq)} + OH^{-} \rightleftarrows \left[Fe(OH)_6\right]^{3-}_{(aq)} + H_2O \quad (7)$$

Hydrolysis of iron (III) nitrate into pure water gave a yellow acid solution with formation of a stable aqueous complex of iron, reaction (1).

Reaction (2) and (3) occurred only after addition of NaOH to the system when the pH was in the range from 0 to 3. Increasing the pH, the complex became a neutral specie, see reaction (4), and the precipitate of ferrihydrite appeared.

Thermodynamically, instability of ferrihydrite at pH>10 favored formation of goethite, α-FeOOH, through the dissolution and recrystallization processes described from (5) to (7).

Iron oxyhydroxide is certainly formed by condensation of aqua-hydroxo ions, performed by olation and oxolation mechanism between OH^- and H_2O ligands, which give rise to Fe-(OH)-Fe and Fe-O-Fe bridges, visible in goethite.

SEM analysis of colloids was carried out after drying on holey carbon film coated copper grid sample holders. It evidenced that all nanoparticles appear composed by smaller rods (Fig. 1), packed in different typical arrangements (rice-grain-like shapes in nanoparticles #1, more squared shapes in #2 and #3), which depend on the synthesis route. The size also depends on the synthesis. In particular, nanoparticles #1 are the largest and #3 the smallest ones, as shown by SEM images (Fig. 1) and DLS measurements (Table 1).

All particles reflect the morphology of crystalline domain (XRD not shown), but with sizes larger of about one order of magnitude, revealing their polycrystalline nature, see Fig. 1 (d-e). The morphology of goethite polycrystalline nanoparticles was strongly influenced by synthesis parameters. Indeed, the processes using TEAH as alkalinizing agent (instead of NaOH), gave nanoparticles with a similar morphology. On the other hand, the procedure of addition of the alkalinizing agent (dropwise or at once, to the solution of iron nitrate), induced growth of

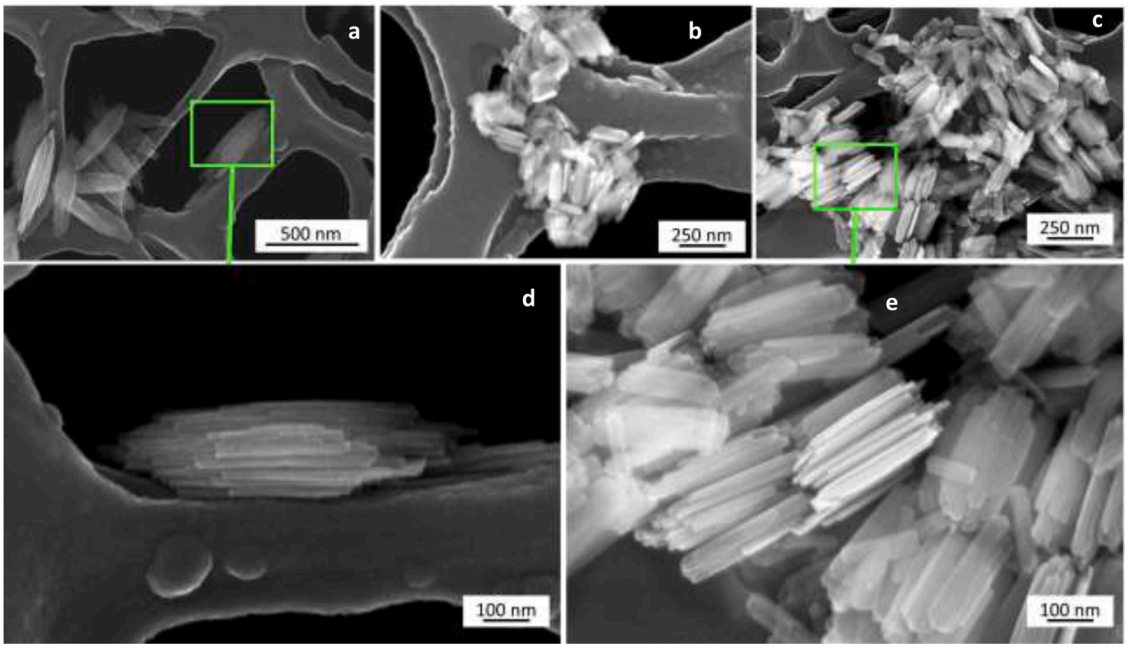

Fig. 1. SEM image of goethite nanoparticles obtained with different synthesis procedures: (a): Sample #1, (b): Sample #2, (c) Sample #3. (d-e): Detail of poly-crystalline nature of single particles.

Table 1
Hydrodynamic sizes obtained by Dynamic Light Scattering (DLS).

Sample	Hydrodynamic size (nm)
#1	261 ± 5
#2	223±2
#3	133±7

pre-existent particles (sample #1 and #2) or the nucleation of new nanoparticles (sample #3). The main difference between NaOH and tetra-ethyl ammonium hydroxide (TEAH) is that the latter is composed of a large cation (tetra-ethyl ammonium) that can adsorb on iron oxides stabilizing them. The initially formed precipitate is completely dissolved on vigorous stirring by using the organic alkali, resulting in homogeneous precipitation conditions for the further synthesis of α-FeOOH with different morphology compared to sample #1.

DLS hydrodynamic size measurements on ferrofluids were repeated several times at the time distance of months. Once dispersed, the still ferrofluids showed sedimentation in few days. However, a simple manual shake restored the original dispersion state, and repeatable DLS sizes were measured (Table 1), demonstrating the absence of clustering or aggregation phenomena.

Morphology and size strongly affect the spectral optical properties of suspensions, firstly investigated in absence of external applied magnetic field. Fig. 2 shows the transmittance spectra of the three samples, normalized to the peak of the highest curve (sample #3) for allowing a better visualization of the spectral differences. All the three samples show three transmittance peaks centered around 910, 1100 and 1260 nm, but with different relative heights and with some shift of the peak maxima. The risefront of the transmittance curves in the range 400–800 nm monotonically increases moving from sample #1 to sample #3 (i.e. considering nanoparticles with decreasing sizes).

Afterwards, magnetic-field-dependent transmittance measurements in the spectral range from the UV (300 nm) to the NIR (1500 nm) were carried with the nanofluids hold in quartz cuvettes of 2 mm path length with a specially designed non-magnetic holder to create magnetic fields of various directions and strengths by means of permanent magnets. The mutual directions of the external magnetic field and the electromagnetic

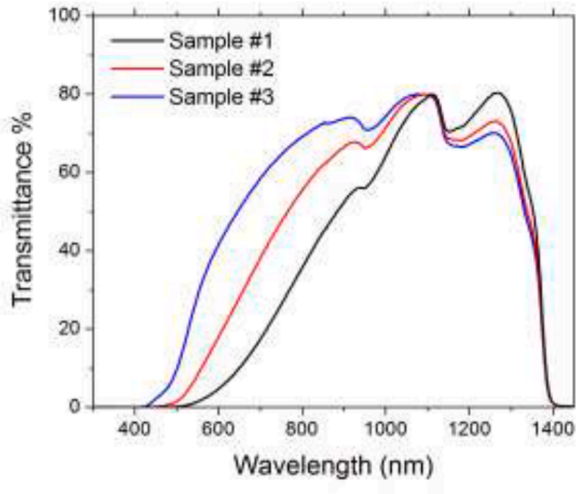

Fig. 2. Transmittance spectra of suspensions, acquired with 2 mm path length. The curves of samples 1 and 2 have been normalized to the highest peak of Sample 3 for an easier comparison of the spectral shapes.

wave vectors considered in the experiments are shown in Fig. 3.

All the three suspensions were sensitive to magnetic fields, which orient the goethite nanorods and modify their optical spectra. The largest sensitivity under external magnetic fields was shown by sample #1. Fig. 4 shows the polarized transmittance spectra acquired for sample #1 under a magnetic field of variable intensity, up to a maximum value $B = 5.60$ mT, applied in different directions with respect to the directions of the electric field (E) and propagation (k) of the probe electromagnetic radiation. For the samples #2 and #3, the sensitivity to the magnetic field is much lower. For them, the differences in transmittance with and without magnetic field (at the maximum value of $B = 5.60$ mT) are within ±2% in absolute transmittance on the peak, which is comparable to the experimental uncertainty of the measurement and therefore not significant to draw conclusions. This lower sensitivity can be due the different nanoparticle shape and size of samples #2 and #3 (as Fig. 2 shows a clear morphology effect on the spectra), even if a

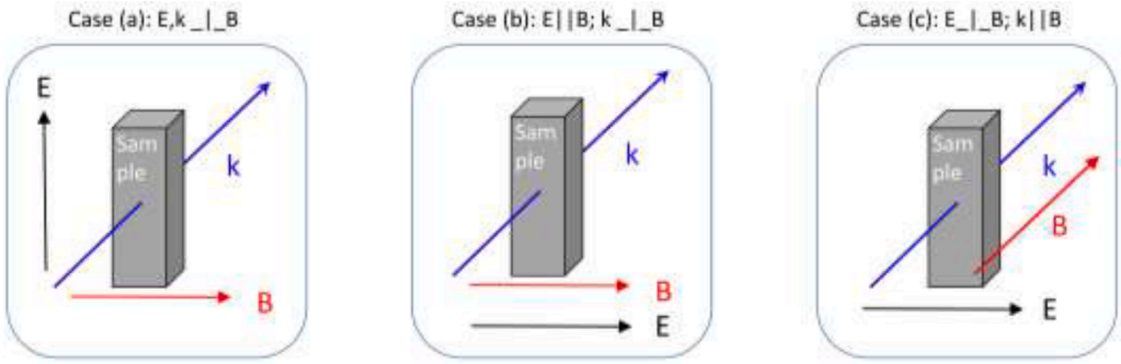

Fig. 3. Sketch of the three cases experimentally considered in this work and mutual directions of involved vectors: applied magnetic field (B), electromagnetic wave polarization (E) and its propagation direction (k).

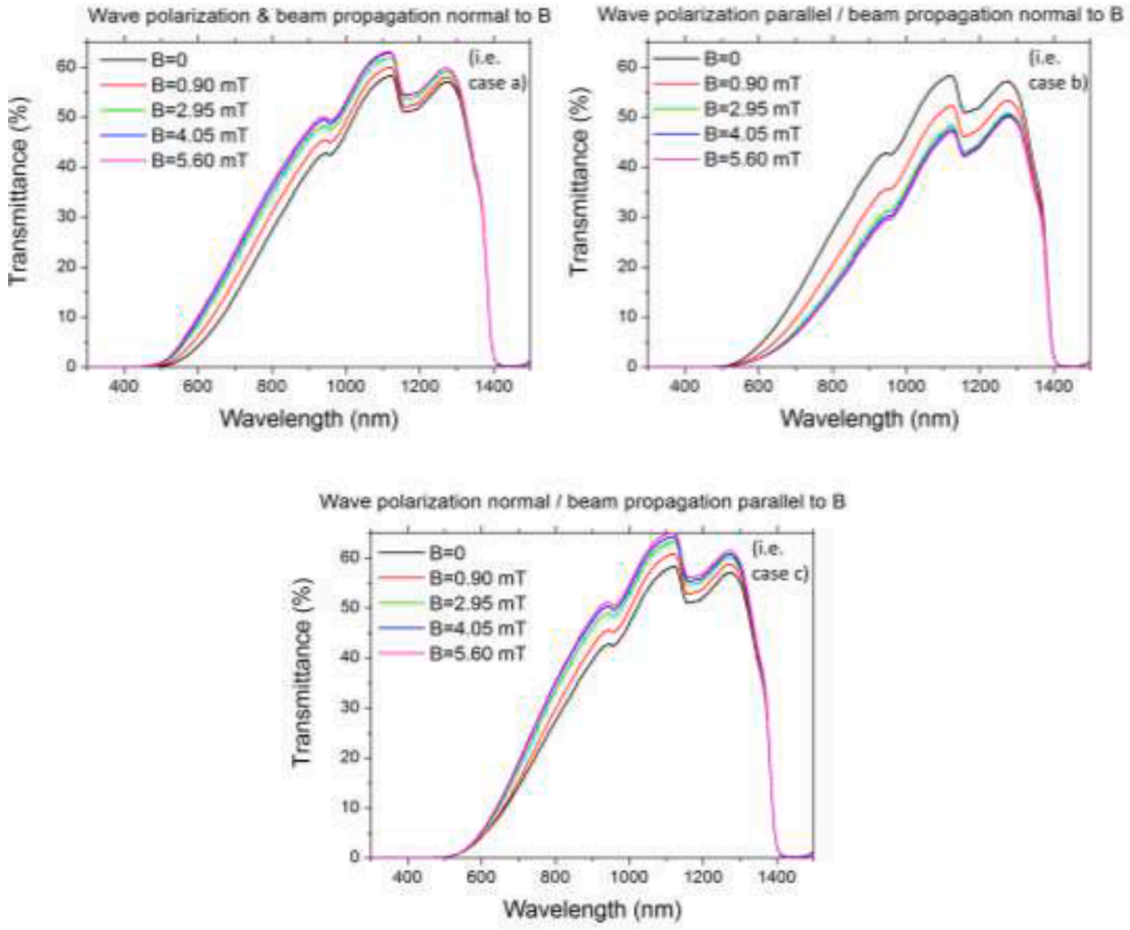

Fig. 4. Magnetic-field-induced changes in the optical transmittance curves of Sample #1. Each plot shows the effect of increasing the value of the magnetic field, for a fixed combination of mutual directions of beam polarization and magnetic field direction. Refer to Fig. 3 for explanation of cases a,b,c.

concentration effect would also concur to amplify the result of sample #1, which is the most concentrated one. Fig. 5 shows an example of bespoke magnetic-field small effects observed in Sample #3.

We observed that the *value* of magnetic-field induced spectral changes in optical transmittance monotonically depends on the strength of the external magnetic field (see Fig. 4, comparing the transmittance curves for three relative directions of the polarization of the beam and applied magnetic field), while their *sign* depends on the relative directions of the external magnetic field and the polarization of the electromagnetic wave (i.e. the transmittance can either increase or decrease, see Fig. 6 comparing the curves with no magnetic field and those acquired at the maximum magnetic field value $B = 5.60$ mT, oriented in different directions and with different polarization directions of the optical beam) [4]. In particular, optical transmittance *increases* under the external magnetic field when the electromagnetic radiation is polarized *perpendicularly* to the magnetic field direction, while the transmittance *decreases* if the polarization of the optical beam is *parallel* to the direction of the magnetic field.

If we consider the difference between the curves acquired *with and without* magnetic field, we see that a spectral range exists where the effect is maximum (i.e. the nanoparticles are not equally sensitive to the magnetic field at all wavelengths). As an example, Fig. 7 shows the

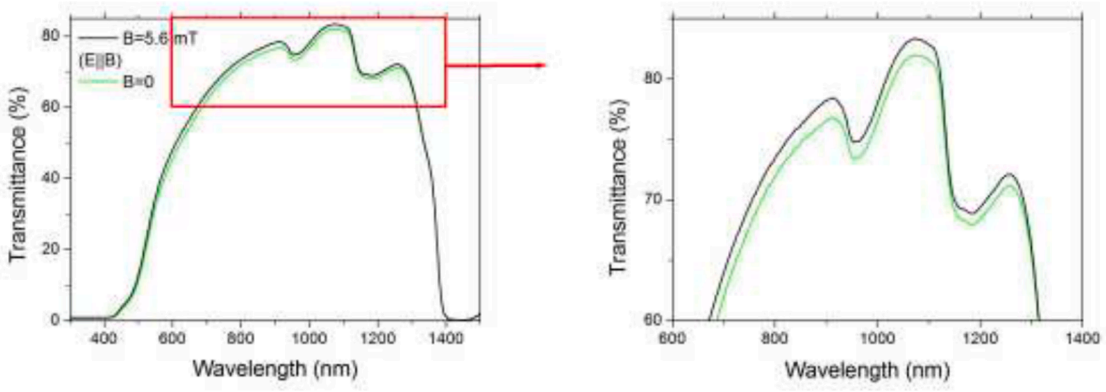

Fig. 5. Effect of magnetic field on Sample #3 (relative directions of vectors as in case (b) in Fig. 3).

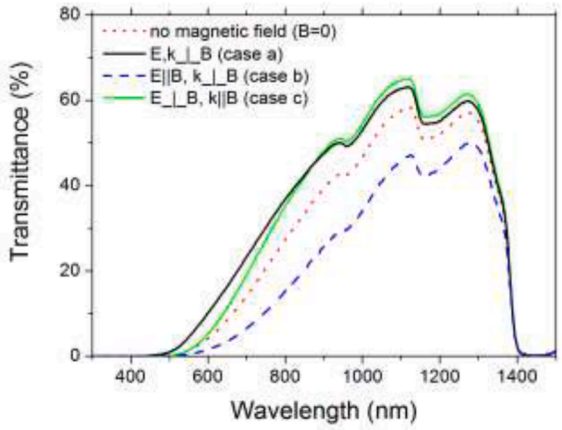

Fig. 6. Effect of the direction of the magnetic field on polarized optical transmittance for fixed magnetic field value $B = 5.60$ mT, for Sample #1. The figure also shows, for comparison, the transmittance in the absence of magnetic field (red dotted curve). Refer to Fig. 3 for explanation of cases a,b,c.

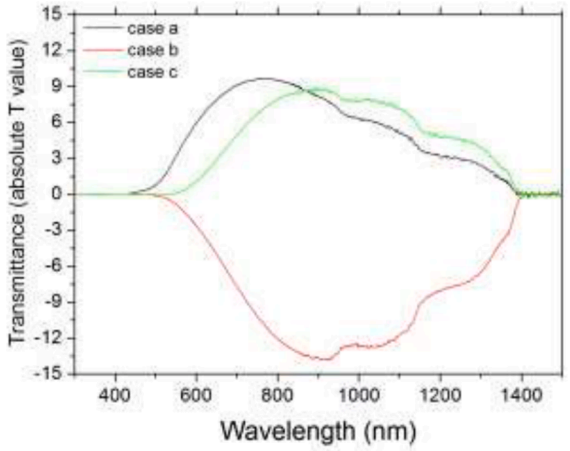

Fig. 7. Differences in the transmittance curves with and without magnetic field, for $B = 5.60$ mT and various mutual directions of light polarization and magnetic field. Refer to Fig. 3 for explanation of cases a,b,c.

transmittance difference with and without magnetic field, at the highest value of magnetic field (5.60 mT) and at the same combinations of mutual directions of light polarization and magnetic field shown in Fig. 4.

From Figs. 4,6,7 we can see that goethite nanoparticles of type #1 can be used as sensors of weak magnetic field. By the change in their transmittance spectra, they are able to discriminate both the absolute value and the direction of the magnetic field. In addition, being their response non-spectrally flat, specific spectral ranges exist where their response is maximized (i.e. where they show the maximum sensitivity, see Fig. 7), which correspond to 763 nm for beam polarization and directions (E normal to B; k normal to B, i.e. case (a) in Fig. 3, positive sign of transmittance change), 905 nm (E normal to B; k parallel to B, i.e. case (c) in Fig. 3, positive sign of transmittance change), 911 nm (E parallel to B, i.e. case b in Fig. 3; negative sign of transmittance change).

Conclusions

Stable aqueous suspensions of goethite nanoparticles were successfully prepared by different synthetic routes, which influenced the morphology and the optical properties of the nanofluids. The external magnetic field was shown to orient the goethite nanoparticles, which behaved like radiation polarizers with tuneable efficiency by changing the magnetic field strength and direction. The optical properties of goethite suspensions depended on their morphology both in the absence of magnetic field and in their response to it. The strongest response was shown by the sample synthesized with route #1, which was also the one with the largest nanoparticles. The other samples #2 and #3 needed additional investigations at higher magnetic field values and/or higher concentrations of nanoparticles. Sample #1 nanoparticles were proved to be very sensitive to both the absolute value and the direction of even weak external magnetic fields (5.60 mT maximum investigated value), with differentiated response as a function of magnetic field value, direction, light polarization and light wavelength. These results open promising perspectives for sensing applications, as well as to realize multi-functional optical/thermal nanofluids (such as in DASCs) with optimized, magnetic-field tailorable, optical and thermal transfer properties [26] by manipulating, through the synthesis processes, the morphology of obtained nanoparticles.

Declaration of Competing Interest

The authors declare that they have no known competing financial interests or personal relationships that could have appeared to influence the work reported in this paper.

Acknowledgments

Authors are grateful to Mr. Mauro Pucci and Mr. Massimo D'Uva (both from CNR-INO) for technical assistance.

References

[1] F. Fang, et al., Facile one-pot preparation of goethite/parabutlerite nanocomposites and their removal properties and mechanism toward As(V) ions, Appl. Surf. Sci. 324 (2015) 355–362, https://doi.org/10.1016/j.apsusc.2014.10.174.

[2] G. Liu, et al., Solid-phase photocatalytic degradation of polystyrene plastic with goethite modified by boron under UV-vis light irradiation, Appl. Surf. Sci. 256 (8) (2010) 2546–2551, https://doi.org/10.1016/j.apsusc.2009.10.102.

[3] M.P. Pomiès, M. Menu, C. Vignaud, Red Palaeolithic pigments: natural hematite or heated goethite? Archaeometry 41 (2) (1999) 275–285, https://doi.org/10.1111/j.1475-4754.1999.tb00983.x.

[4] E. Sani, L. Mercatelli, M.R. Martina, S. Barison, F. Agresti, Magnetic-field tunability of optical properties in colloidal suspensions of goethite (α-FeOOH) nanorods, Opt. Mater. (Amst). 96 (Oct. 2019), 109303, https://doi.org/10.1016/j.optmat.2019.109303.

[5] B.J. Lemaire, et al., Physical properties of aqueous suspensions of goethite (α -FeOOH) nanorods: part I: in the isotropic phase, Eur. Phys. J. E 13 (3) (2004) 291–308, https://doi.org/10.1140/epje/i2003-10078-6.

[6] F. Agresti, et al., NIR transmittance tuneability under a magnetic field of colloidal suspensions of goethite (α-FeOOH) nanorods, RSC Adv. 7 (20) (2017), https://doi.org/10.1039/c7ra00721c.

[7] B.J. Lemaire, et al., The complex phase behaviour of suspensions of goethite (α-FeOOH) nanorods in a magnetic field, Faraday Discuss. 128 (2005) 271–283, https://doi.org/10.1039/b403074e.

[8] B.J. Lemaire, et al., Outstanding magnetic properties of nematic suspensions of goethite ($\ensuremath{\alpha}$-FeOOH) Nanorods, Phys. Rev. Lett. 88 (12) (Mar. 2002), 125507, https://doi.org/10.1103/PhysRevLett.88.125507.

[9] M. Nazari, M.H. Rasoulifard, H. Hosseini, Dielectric breakdown strength of magnetic nanofluid based on insulation oil after impulse test, J. Magn. Magn. Mater. 399 (2016) 1–4.

[10] P.D. Shima, J. Philip, Tuning of thermal conductivity and rheology of nanofluids using an external stimulus, J. Phys. Chem. C 115 (2011) 20097–20104.

[11] M. Bahiraei, M. Hangi, Flow and heat transfer characteristics of magnetic nanofluids: a review, J. Magn. Magn. Mater. 374 (2015) 125–138.

[12] N. Çobanoğlu, A. Banisharif, P. Estellé, Z.H. Karadeniz, The developing flow characteristics of water-ethylene glycol mixture based Fe_3O_4 nanofluids in eccentric annular ducts in low temperature applications, Int. J. Thermofluids 14 (2022), 100149.

[13] E. Seid, E. Haile, T. Walelign, Multiple slip, Soret and Dufour effects in fluid flow near a vertical stretching sheet in the presence of magnetic nanoparticles, Int. J. Thermofluids 13 (2022), 100136.

[14] Z. Hedayatnasab, F. Abnisa, W.M.A.W. Daud, Review on magnetic nanoparticles for magnetic nanofluid hyperthermia application, Mater. Des. 123 (2017) 174–196.

[15] R.A. Revia, M. Zhang, Magnetite nanoparticles for cancer diagnosis, treatment, and treatment monitoring: recent advances, Mater. Today 19 (2016) 157–168.

[16] E. Rodríguez-Schwendtner, N. Díaz-Herrera, M.C. Navarrete, A. González-Cano, Ó. Esteban, Plasmonic sensor based on tapered optical fibers and magnetic fluids for measuring magnetic fields, Sens. Actuators A Phys. 264 (2017) 58–62.

[17] H.E. Horng, et al., Tunable optical switch using magnetic fluids, Appl. Phys. Lett. 85 (2004) 5592–5594.

[18] Z. Liu, Y. Yan, R. Fu, M. Alsaady, Enhancement of solar energy collection with magnetic nanofluids, Therm. Sci. Eng. Prog. 8 (Dec. 2018) 130–135, https://doi.org/10.1016/j.tsep.2018.08.015.

[19] T.J. Salez, et al., Can charged colloidal particles increase the thermoelectric energy conversion efficiency? Phys. Chem. Chem. Phys. 19 (14) (Apr. 2017) 9409, https://doi.org/10.1039/c7cp01023k.

[20] E. Sani, M.R. Martina, T.J. Salez, S. Nakamae, E. Dubois, V. Peyre, Multifunctional magnetic nanocolloids for hybrid solar-thermoelectric energy harvesting, Nanomaterials 11 (2021) 1031.

[21] R. Mulka, B. Zajączkowski, E. Neuber, M.H. Buschmann, Contact angle of the ferronanofluid and influence of the magnetic field on the drying droplet, Int. J. Thermofluids 14 (2022), 100152.

[22] S. Hinrichs et al., "Goethite nanorods: synthesis and investigation of the size effect on their orientation within a magnetic field by SAXS," doi: 10.3390/nano10122526.

[23] S. Zeng, K. Tang, T. Li, Controlled synthesis of α-Fe_2O_3 nanorods and its size-dependent optical absorption, electrochemical, and magnetic properties, J. Colloid Interface Sci. 312 (2) (2007) 513–521, https://doi.org/10.1016/j.jcis.2007.03.046.

[24] M. Kosmulski, S. Durand-Vidal, E. Maczka, J.B. Rosenholm, Morphology of synthetic goethite particles, J. Colloid Interface Sci. 271 (2) (2004) 261–269, https://doi.org/10.1016/j.jcis.2003.10.032.

[25] Y. Cudennec, A. Lecerf, The transformation of ferrihydrite into goethite or hematite, revisited, J. Solid State Chem. (2006) 716–722.

[26] I. Nkurikiyimfura, Y. Wang, Z. Pan, Effect of chain-like magnetite nanoparticle aggregates on thermal conductivity of magnetic nanofluid in magnetic field, Exp. Therm. Fluid Sci. 44 (2013) 607–612.